Threshold criteria for undervoltage breakdown

James E. Cooley[a] and Edgar Y. Choueiri[b]
Electric Propulsion and Plasma Dynamics Laboratory, Princeton University, Princeton, New Jersey 08544, USA

(Received 27 September 2007; accepted 28 February 2008; published online 8 May 2008)

The conditions under which an externally supplied pulse of electrons will induce breakdown in an undervoltaged, low-gain discharge gap are experimentally and theoretically explored. The minimum number of injected electrons required to achieve breakdown in a parallel-plate gap is measured in argon at *pd* values of 3–10 Torr m using ultraviolet laser pulses to photoelectrically release electrons from the cathode. This value was found to scale inversely with voltage at constant *pd* and with pressure within the parameter range explored. A dimensionless theoretical description of the phenomenon is formulated and numerically solved. It is found that a significant fraction of the charge on the plates must be injected for breakdown to be achieved at low gain. It is also found that fewer electrons are required as the gain due to electron-impact ionization (α process) is increased, or as the sensitivity of the α process to electric field is enhanced by increasing the gas pressure. A predicted insensitivity to ion mobility implies that the breakdown is determined during the first electron avalanche when space-charge distortion is greatest. © *2008 American Institute of Physics*. [DOI: 10.1063/1.2913196]

I. INTRODUCTION

Undervoltage breakdown is the phenomenon in which a burst of electrons at the cathode of a discharge gap that is held below its breakdown voltage leads to a discharge. Such a system is analogous to any of a wide variety of natural systems that demonstrate local stability with a finite activation barrier; the nonconducting state is stable to small perturbations, but the injection of a certain threshold amount of charge lifts the system across the barrier and a conducting state is reached. This work explores the physical processes that determine the magnitude of that activation barrier in order to uncover fundamental insight into the phenomenon.

Aside from its value as a fundamental question, undervoltage breakdown is relevant to gas avalanche particle detectors[1] and in several high-current switching applications such as discharge initiation in pulsed plasma thrusters,[2] and pseudospark switches.[3] The phenomenon is qualitatively similar to oscillations in dc-driven barrier discharges,[4,5] in which pulses of current produced during breakdowns are deposited on semiconductor layers, altering the distribution of space charge and temporarily suppressing conductivity.

The phenomenon was first observed experimentally by Kluckow[6] as reported by Raether.[7] Work was carried out by others,[8,9] most extensively Sato and Sakamoto, who investigated the phenomenon in air, theoretically and experimentally, over a range of pressures. Fonte[10] modeled the breakdown of parallel-plate avalanche chambers and showed that the breakdown threshold—the minimum criteria under which breakdown will occur in those devices, corresponds to the conditions necessary for streamer formation—predicted by Raether as described in his textbook.[7] This result is consistent with experimental measurements of breakdown threshold in parallel-plate avalanche chambers for a variety of conditions.[1]

That work described well the breakdown behavior in such high-gain ($e^{\alpha_0 d}$ greater than about 10^4) devices in which bursts of electrons are likely to grow to the point of streamer formation. However, the literature contains numerous examples of undervoltage breakdown through a Townsend-type, or "slow" breakdown mechanism at lower gain, in which breakdown is achieved through the buildup of successively larger generations of avalanches enhanced by space-charge effects. Yet, no discussion of threshold criteria for such a phenomenon has been reported. This is the primary focus of this work—we will both experimentally measure and theoretically calculate the critical injected charge required to achieve breakdown in an undervoltaged discharge gap, and explore the dependencies of this value on relevant experimental parameters so as to achieve a fundamental understanding of the physical mechanisms that govern this phenomenon.

The term "breakdown," used frequently in this work, is intended to refer in general to a transition from a nonconducting to a conducting state. In most cases, we use the term to refer to the transition from a Townsend to a glow discharge.

In Sec. II, we present the results of an experiment designed to measure the critical charge required for undervoltage breakdown. The discharge is achieved in a parallel-plate discharge gap through the injection of electron pulses resulting from laser pulses directed onto a photoemissive target fixed to the cathode. Argon is used at a relatively low pressure (on the order of 1 Torr) and the experimentally observed breakdown time scale implies the prominence of the Townsend mechanism.

Section III contains a formulation of a dimensionless theoretical description of undervoltage breakdown. The pri-

[a]Electronic mail: cooley@princeton.edu.
[b]Electronic mail: choueiri@princeton.edu.

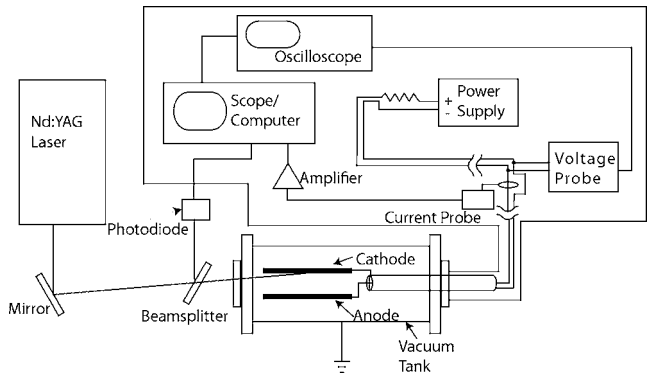

FIG. 1. Schematic of the undervoltage breakdown experiment.

mary aim of this theoretical work is to find the simplest model that explains the observed experimental trends in critical injected density. As such, we make a number of simplifying assumptions that allow us to clarify the most relevant mechanisms at work in our experimental arrangement. We then explore, to the extent that those assumptions hold, the dependencies of this value on various parameters (gas pressure, voltage, gap width, ion mobility, secondary emission coefficient).

Finally, in Sec. IV, we will discuss a number of physical insights gleaned from examination of the experimental and theoretical results.

II. EXPERIMENT

The experiment is designed to measure the minimum injected charge required to achieve undervoltage breakdown for a given set of initial conditions. Intended to be as simple as possible for phenomenological clarity, the apparatus is a parallel-plate discharge gap and argon is used as the working gas.

A. Experimental setup and methods

Figure 1 is a schematic of the experimental setup. A pulsed laser is directed through a beamsplitter which reflects a small fraction (approximately 1%) of the beam onto a photodiode. We use a Q-switched Nd:YAG at its fourth harmonic of 266 nm, a pulse width of 10 ns, and a maximum energy of 4 mJ—not enough to significantly heat the surface so that electron emission is presumed to result from the photoelectric effect. The beam passes through the window of a vacuum chamber and onto an oxygen-free high-conductivity (OFHC) copper target fixed to the cathode of a pair of parallel-plate electrodes, separated by a gap width of 2.54 cm. The beam has a spot diameter of 8 mm and intercepts the cathode surface at an angle of 20°. The chamber is evacuated to a pressure of 10^{-9} Torr, then filled with argon to the desired pressure, ranging from 1–3 Torr. A voltage-regulated power supply maintains a static potential across the electrodes, which float with respect to the ground. Current signals are carried out from the plates by way of a 50 Ω transmission line and are measured by an inductive current transformer, whose signal is amplified and recorded on a Tektronix 5104b oscilloscope, which also measures the photodiode signal. The voltage across the plates is measured and recorded by a separate oscilloscope. All measurement electronics sit inside a grounded Faraday cage that isolates them from electromagnetic noise. The system is run by an automated Labview data acquisition system.

The breakdown voltage is measured several times to an accuracy of about 2%; then, a desired undervoltage is applied across the plates. Because ionization avalanching amplifies the initial electron pulse in the presence of gas, we performed an *a priori* vacuum calibration, correlating the charge released with the intensity of the laser pulse. In the presence of gas, measurement of the laser intensity thus allowed us to calculate the initial charge released.

Figure 2 contains examples of the oscilloscope traces used to calculate the threshold curves. For each laser firing, one set of photodiode and voltage traces is recorded and analyzed. The time scales on the two traces are different; a laser pulse would appear as instantaneous at $t=0$ on the voltage trace. The traces in Fig. 2(a) represent a relatively weak

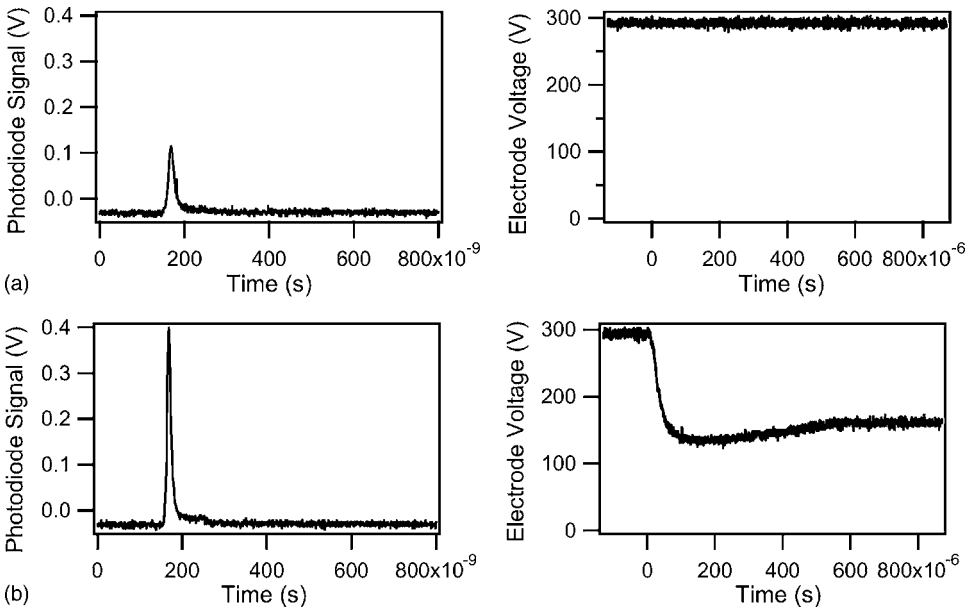

FIG. 2. Two pairs of oscilloscope traces recorded in the undervoltage breakdown experiment. These were taken with argon at 3 Torr, and an initial electrode voltage of 295 V.

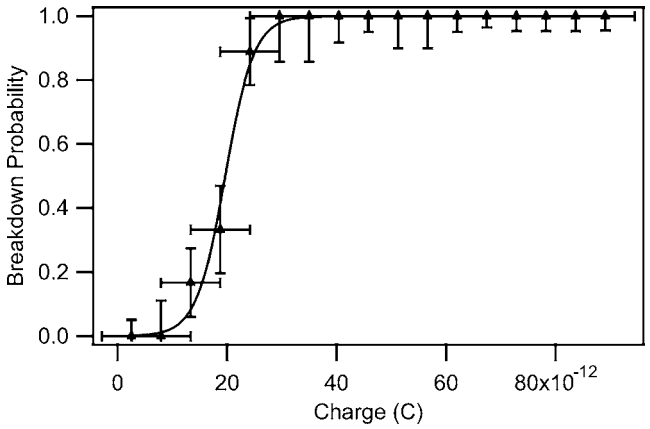

FIG. 3. Probability of breakdown as a function of charge in the initial pulse for argon at 3 Torr and 295 V. A least-squares fit of Eq. (1) is overlaid.

laser pulse that does not result in a breakdown; no change in voltage is observed. In Fig. 2(b), however, a more intense pulse does result in breakdown. This is manifested in a drop in voltage across the electrodes. Such a voltage drop always corresponds to the formation of visible plasma between the electrodes. Note the time scale of the voltage drop, on the order of 10 microseconds. Such a timescale corresponds to several ion transit times (on the order of 1 μs), implying that Townsend, not streamer, breakdown is at work.

For each photodiode trace, the small dc offset is subtracted and the maximum value is recorded. The corresponding voltage trace is then analyzed to determine if a breakdown occurred. A weighted histogram is then calculated which divides the entire range of charge values into bins and specifies the fraction of shots within each bin that resulted in a breakdown.

B. Results

Such a histogram is plotted in Fig. 3. Charge error bars come from the vacuum pulse calibration and represent the root-mean-square deviation of charges for a given photosignal bin. Error bars on the probability are calculated based on binomial error, $\sigma=\sqrt{p(1-p)/n}$, where p is the fraction of times a pulse in that charge bin caused a breakdown and n is the number of pulses in the bin.

We see that, at very low values of initial charge, breakdown is very unlikely; at very high values, breakdown is very likely, and some intermediate regime exists. The quantity we are seeking, the number of electrons (or the total charge) in a pulse required to achieve undervoltage breakdown, can be gleaned from graphs such as this.

We fit the data to sigmoid functions of the form

$$y(x)=\frac{1}{1+\exp\left(\frac{x_{1/2}-x}{\nu}\right)}, \tag{1}$$

which assumes that $y(x)$ reaches unity as $x\to\infty$ and vanishes as $x\to 0$. $x_{1/2}$ represents the charge value at which the breakdown probability is 50%. We will define this value as the threshold charge and plot it for varied experimental conditions. Because of the steepness of the breakdown probability curves, the results are insensitive to the definition of threshold charge.

In Fig. 4, we show the experimentally measured threshold charge as a function of V/V_b (plate voltage normalized to the breakdown voltage at each pressure) for argon at pressures of 1.6, 2, and 3 Torr. Error bars represent the error on the fit parameter $x_{1/2}$ from Eq. (1). Least-squares fits of all data sets yielded χ^2/M, where M is the number of relevant degrees of freedom, ranging from about 0.5 to 1.

The results demonstrate a trend of decreasing threshold charge with increasing pressure and, at least at lower pressure values, with increasing voltage. The experiment was also carried out at pressures of 1.5, 1.4, and 1 Torr, but no breakdowns occurred at these lower pressures.

III. THEORY

A. Formulation

We now seek to find the simplest model that demonstrates the observed experimental trends, so we treat one-dimensional discharge gaps with nonattaching gases in which secondary emission is only through ion impact and is field independent. We also adopt the assumptions that the mobilities are field independent and that diffusion and particle loss are negligible. Use of these assumptions allows us to describe the problem with a relatively small number of dimensionless parameters.

Of course, one could consider a variety of extensions to this model, exploring the roles of field-dependent or photon-based secondary emission, multidimensional effects, field-dependent mobilities, attachment, diffusion, loss, or nonlocal ionization rates as appropriate for a specific application. Our idealized approach in this work could thus serve as a starting

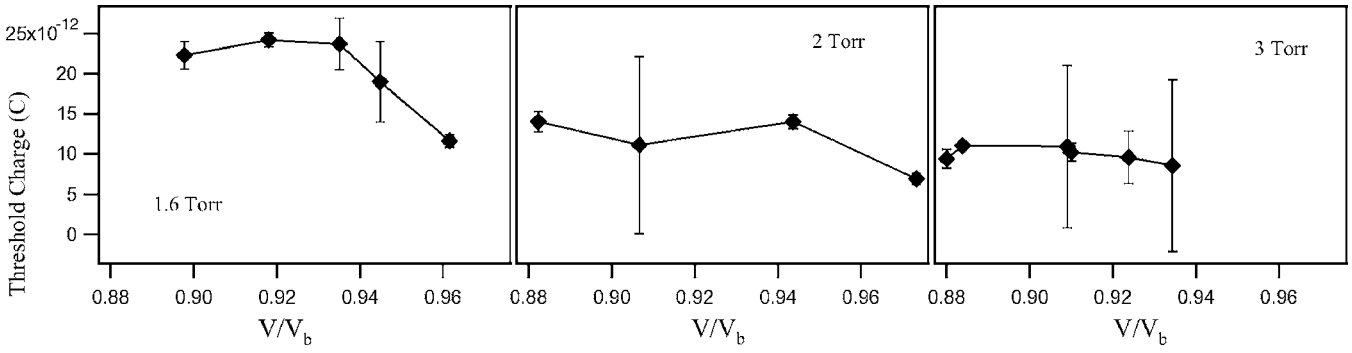

FIG. 4. Threshold charge as measured by the undervoltage breakdown experiment in argon at 1.6, 2, and 3 Torr.

point for such future efforts. In particular, the experiment is clearly not one-dimensional; while the parallel-plate electrodes provide a uniform electric field, and insulating coating isolates the discharge in the center of the electrode area far from the fringing fields at the edges, the laser does not uniformly illuminate the entire cathode area. Instead, the angle of incidence of the laser is such that the irradiated area is elliptical and roughly 2.3 cm long by 0.8 cm wide. Such a distribution is smaller than the total area of the electrodes, which have 5×5 cm of exposed surface. However, each dimension of the discharge is longer than the free-diffusion length of an electron during a single-electron avalanche transit (about 1 mm). Thus, multidimensional, diffusion-based analyses, such as that employed by Raether[7] and others in calculating streamer formation as started from a single electron, are not required. A 1D analysis, while not completely accurate, should capture the essence of the most important physical processes.

In addition, we expect a field-dependent γ and photoelectric secondary emission to play large roles in undervoltage breakdown for contaminated cathodes and discharges of low E/p.

Our formulation begins with the fluid-based approach employed in the "classical model" for glow discharges that was originally presented by von Engel and Steenbeck[11] but treated by many other authors (see, for example, Refs. 7, 12, and 13). The governing equations are continuity equations for electrons and singly charged ions and Poisson's equation,

$$\frac{dn_e}{dt} = \alpha\Gamma_e - \frac{d}{dx}\Gamma_e, \tag{2}$$

$$\frac{dn_+}{dt} = \alpha\Gamma_e + \frac{d}{dx}\Gamma_+, \tag{3}$$

$$\frac{d^2\phi}{dx^2} = \frac{-e}{\epsilon_0}(n_+ - n_e), \tag{4}$$

$$E = -\frac{d\phi}{dx}. \tag{5}$$

We assume that the velocities of electrons and ions are the drift velocities so that $\Gamma_{e,+}=n_{e,+}\mu_{e,+}E$ is the flux of each respective species. If we define $x=0$ as the cathode position and $x=d$ as the anode, then the governing equations are subject to the boundary conditions,

$$\phi(0,t) = 0, \tag{6}$$

$$\phi(d,t) = V, \tag{7}$$

$$\Gamma_e(0,t) = \gamma\Gamma_+(0,t) + \Gamma_{\text{pulse}}(t). \tag{8}$$

Equations (6) and (7) state that the potential difference across the electrodes is held at the applied voltage. Equation (8) is the boundary condition for electron flux and the cathode, and includes secondary emission from the cathode from ions and photons. γ is the secondary emission coefficient from ion impact on the cathode. We neglect secondary emission due to photon impact. The cathode boundary condition treats the external pulse of electrons,

$$\Gamma_{\text{pulse}}(t) = \frac{N_{e0}}{\tau\sqrt{\pi}}e^{-[(t-3\tau)/\tau]^2}, \tag{9}$$

where τ is the time width of the pulse and N_{e0} is the total number of electrons per unit area to be released during the duration of the pulse. We assume that secondary ion emission due to electron impact at the anode is negligible, so that the inward flux of ions at the anode is zero,

$$\Gamma_+^{in}(x=d) = 0. \tag{10}$$

We use the classical form for Townsend's first coefficient,[12]

$$\alpha(|E|) = Ape^{-Bp/|E|}, \tag{11}$$

where A and B are empirically determined, gas-dependent coefficients, p is the neutral pressure, and E is the local electric field.

TABLE I. Dimensional variables and reference quantities used in the calculation.

Dimensional quantity q	Description	Reference quantity q'
α	Ionization coefficient	$\alpha'=\alpha_0=Ape^{-(Bpd/V)}$
x	Position coordinate	$x'=\frac{1}{\alpha_0}$
d	Gap width	x'
E	Electric field	$E'=V/d$
$\mu_{e,+}$	Mobility	μ_e
$v_{e,+}$	Velocity	$v'=\mu_e\frac{V}{d}$
t	Time	$t'=x'/v'$
τ	Temporal pulse width	t'
$n_{e,+}$	Particle density	$n'=\alpha_0 N_{e0}$
p	Neutral pressure	$p'=\frac{V}{Bd}$
N_{e0}	Electron pulse density	$N'=\frac{V\epsilon_0}{ed}$
ϕ	Electrostatic potential	$\phi'=\frac{V}{\alpha_0 d}$
$\Gamma_{e,+}$	Particle flux	$\Gamma'=n'v'$

1. Nondimensionalization

We normalize each variable, q, to a reference variable, q', to form a nondimensional parameter, $\bar{q}$, such that

$$\bar{q} \equiv \frac{q}{q'}. \tag{12}$$

The relevant variables and their normalizations are listed in Table I.

The dimensionless pressure $\bar{p}$ is essentially the inverse of the applied reduced field E/p.

The dimensionless governing equations are

$$\frac{d\bar{n}_e}{d\bar{t}} = \bar{\alpha}\bar{n}_e\bar{E} - \frac{d}{d\bar{x}}\bar{n}_e\bar{E}, \tag{13}$$

$$\frac{d\bar{n}_+}{d\bar{t}} = \bar{\alpha}\bar{n}_e\bar{E} + \frac{d}{d\bar{x}}\bar{n}_+\bar{\mu}_+\bar{E}, \tag{14}$$

$$\frac{d^2\bar{\phi}}{d\bar{x}^2} = -\bar{N}_{e0}(\bar{n}_+ - \bar{n}_e), \tag{15}$$

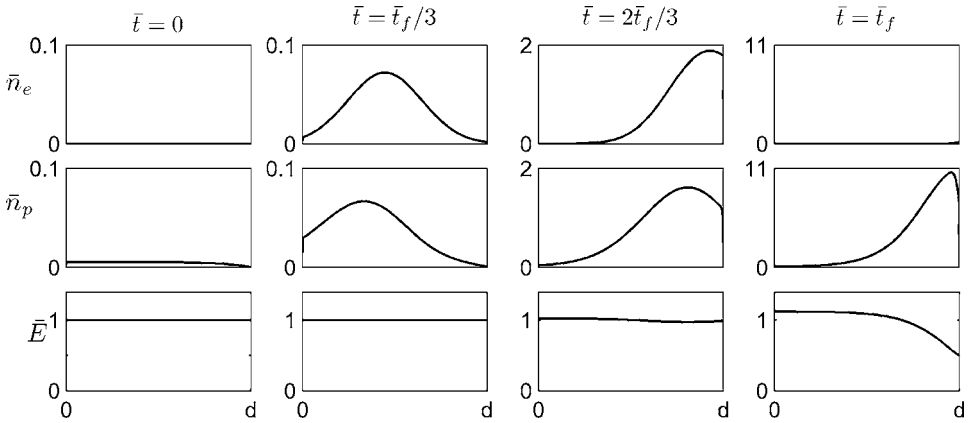

FIG. 5. Time-dependent variation of normalized electron density, ion density, and electric field at various times during the initial electron avalanche transit. Here, $\bar{p}=2.15$, $\alpha_0 d=7$, and $\bar{N}_{e0}=4\times10^{-2}$. Note the scale changes on the density plots.

$$\bar{E}=-\frac{d\bar{\phi}}{d\bar{x}},$$

$$\bar{\alpha}=\exp[\bar{p}(1-1/\bar{E})]. \tag{16}$$

The boundary conditions [Eqs. (6)–(10)] become

$$\bar{\phi}(0,\bar{t})=0, \tag{17}$$

$$\bar{\phi}(\bar{d},\bar{t})=\bar{d}, \tag{18}$$

$$\bar{\Gamma}_e(0,t)=\gamma\bar{\Gamma}_+(0,\bar{t})+\frac{\bar{N}_{e0}}{\bar{\tau}\sqrt{\pi}}e^{-[(\bar{t}-3\bar{\tau})/\bar{\tau}]^2}. \tag{19}$$

Taking into account the possibility of a nonuniform electric field, we write Townsend's well-known breakdown criterion as

$$M=\gamma\{\exp[\int_0^d\alpha(x)dx]-1\}\geq 1. \tag{20}$$

In undervoltage breakdown, we choose $M<1$ as an initial condition. Since we neglect the dependence of γ on electric field, we can interpret the phenomenon as an increase in M resulting from an increase in $\int_0^d\alpha(x)dx$ (though we will see that raising M above unity is a necessary but not sufficient criterion for breakdown).

The temporal pulse width should have no effect as long as it is much less than the electron transit time. In addition, we assume that $\bar{\mu}_+=\mu_+/\mu_e$ is constant, an assertion that is true if both mobilities have the same pressure scaling and are independent of electric field. The problem is therefore uniquely specified with five dimensionless parameters,

$$\bar{N}_{e0}=\frac{N_{e0}ed}{\epsilon_0 V} \qquad M_0=\gamma(e^{\alpha_0 d}-1)$$

$$\gamma \qquad \bar{\mu}_+=\frac{\mu_+}{\mu_e} \qquad \bar{p}=\frac{B}{E_0/p}$$

We thus aim to find, for a given M_0, $\bar{p}$, γ, and $\bar{\mu}_+$, the minimum $\bar{N}_{e0}$ that will result in breakdown.

B. Solution and results

1. Solution method

We treat the problem on two time scales. Fine time steps are used during the transit of the first electron avalanche so that electron dynamics during the pulse injection can be accurately described. Coarser time steps are then used to describe ion dynamics during subsequent avalanches. Time steps are dynamically calculated to satisfy the Courant-Friedrich-Levy stability condition,[14]

$$\Delta\bar{t}=\frac{\Delta\bar{x}}{\max|\bar{v}|}\nu, \tag{21}$$

where ν, the Courant number, is held at a fixed value of 0.95. The relevant wave speed during the electron pulse transit is the electron drift velocity, but the ion drift velocity is used thereafter. On the ion time scale, we calculate the electron flux by replacing Eq. (13) with the approximation

$$\bar{\Gamma}_e(\bar{x},\bar{t})=\bar{\Gamma}_e(0,\bar{t})\exp\int_0^{\bar{x}}\bar{\alpha}(\bar{x},\bar{t})d\bar{x}. \tag{22}$$

This approximation is valid provided that the electron flux from the cathode does not change significantly during an electron transit time, which is the case for most of the breakdown process, but that does not hold during the injection of the electron pulse.

We solve Eqs. (13)–(16) numerically using a 1D time-dependent finite-volume method.[14] Equations (13) and (14) are advection-reaction equations and are solved using an upwind scheme so that, at the $m$thth time step at position i,

$$n_i^m=n_i^{m-1}-\frac{v\Delta\bar{t}}{\Delta\bar{x}}(n_i^{m-1}-n_{i-1}^{m-1})+\Delta\bar{t}\alpha_i^{m-1}\bar{v}_e\bar{n}_e, \tag{23}$$

where n is either the nondimensional ion or electron density and v is the relevant nondimensional drift velocity.

Poisson's Eq. (15) is solved subject to the boundary conditions Eqs. (17) and (18) at every time step using a tridiagonal inversion method.[15]

C. Theoretical results

In Fig. 5 we plot the normalized electron and ion densities and electric field during the first avalanche transit. Introduced at the cathode, the electron pulse drifts across the gap,

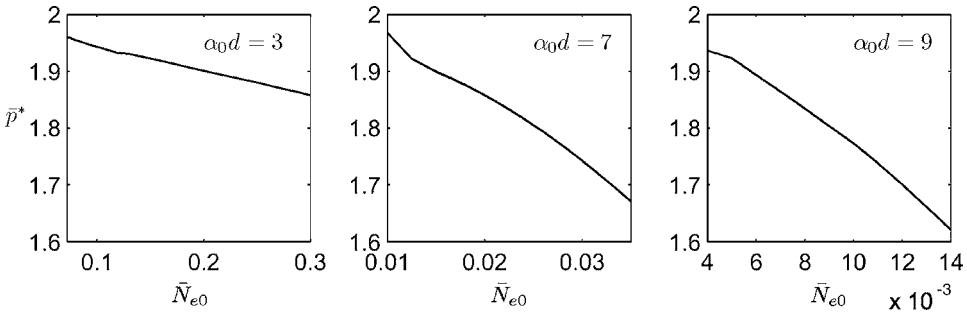

FIG. 6. Critical $\bar{p}$ as a function of injected pulse size and gain factor.

grows due to ionizing collisions, then exits at the anode. The ions it created are left behind due to their lower mobility and the resulting charge imbalance distorts the electric field, enhancing it near the cathode but suppressing it near the anode.

Based on von Engel's and Steenbeck's[11] well-known analysis of the current-voltage characteristic of the cathode fall of a stationary glow discharge, in which $\alpha''(E)=0$ is designated as a critical point for space-charge distortion, one would expect undervoltage breakdown to be impossible in the so-called "supercritical" parameter regimes. That is, if $E/p > B/2$ (or, equivalently, $\bar{p} < 2$), it might be expected that the net effect of the space-charge distortion of our injected pulse will be to reduce the overall degree of ionization and breakdown will not occur. Such a supposition would nearly be true, save for the precise designation of the critical point.

In fact, that analysis employs a second-order expansion of the electric field perturbation, an approach that is valid when the space-charge distortion is small. In Ref. 13, however, a higher-order analysis demonstrates that the transition to supercritical behavior does not necessarily coincide with the condition that $\alpha''=0$ for large space-charge distortions. Instead, higher-order distortions suppress the pd values at which this critical transition occurs. For the large distortion induced by the injected electron pulses in an undervoltage breakdown event, the critical value of E/p depends, therefore, on the magnitude of the injected pulse and the ionization gain of the discharge gap. Figure 6 plots calculated values of this critical parameter, here expressed as $\bar{p}^*$, a critical value of $\bar{p}$, as a function of $\bar{N}_{e0}$ and $\alpha_0 d$. Indeed, we find that the critical values of $\bar{p}$ occur below those predicted by a second-order analysis. This is consistent with the results of Ref. 13.

For convenience, we introduce a dimensionless time parameter,

$$\xi \equiv \frac{t}{T_+ + T_e}, \tag{24}$$

where $T_{+,e}=d/(\mu_{+,e}E_0)$ are the transit times of the ions and electrons as a result of the unperturbed field. In the absence of space-charge effects, 1 ξ would be the duration of one avalanche generation.

We plot the normalized ion density distribution as a function of ξ for two cases: in Fig. 7 an injected electron pulse that is not large enough to cause breakdown and in Fig. 8 a larger pulse which does cause breakdown. The first electron avalanche appears instantaneous on this time scale, so the initial condition is the ion distribution resulting from that avalanche. The ions drift toward the cathode ($\bar{x}=0$), releasing second-generation electrons due to secondary emission. Those electrons instantaneously result in second-generation ions, which in turn drift toward the cathode, producing further avalanche generations. Since $M<1$ is always an initial condition, we expect each generation to be smaller than the previous in the absence of space-charge distortion. In the first case (Fig. 7) this behavior is evident, as successive avalanches gradually die out in magnitude. In the second case (Fig. 8), however, the space-charge distortion is large enough

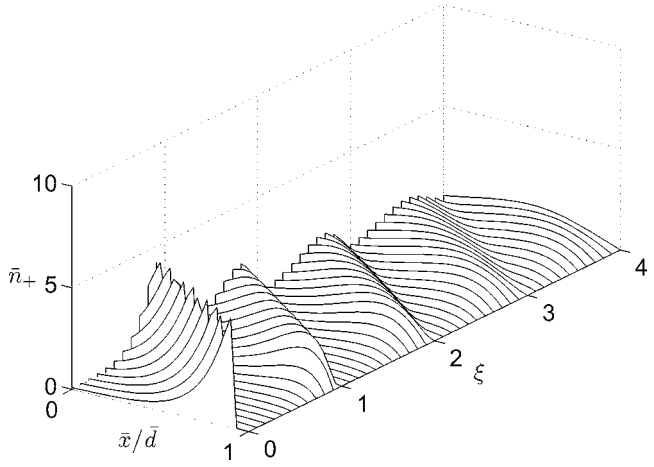

FIG. 7. Normalized ion density distribution as a function of ξ for $\bar{p}=2.15$, $M_0=0.95$, $\gamma=7.13\times10^{-4}$, $\bar{\mu}_+=0.004$, and $\bar{N}_{e0}=5\times10^{-3}$. The avalanche generations gradually die out and no breakdown will occur.

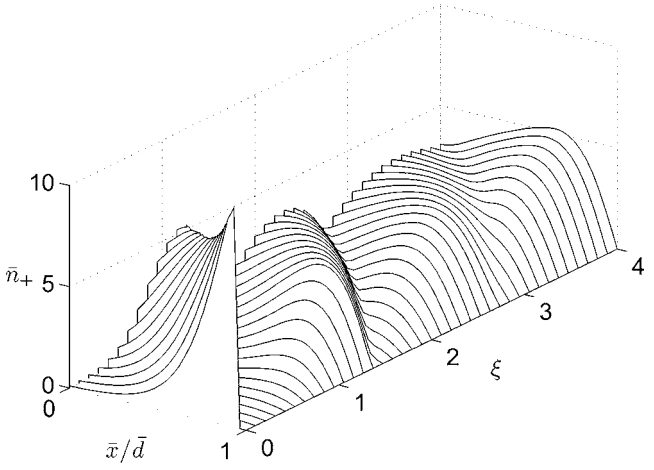

FIG. 8. Normalized ion density distribution as a function of ξ for $\bar{p}=2.15$, $M_0=0.95$, $\gamma=7.13\times10^{-4}$, $\bar{\mu}_+=0.004$, and $\bar{N}_{e0}=1.5\times10^{-2}$. Here, the avalanches build in magnitude; a breakdown will eventually result.

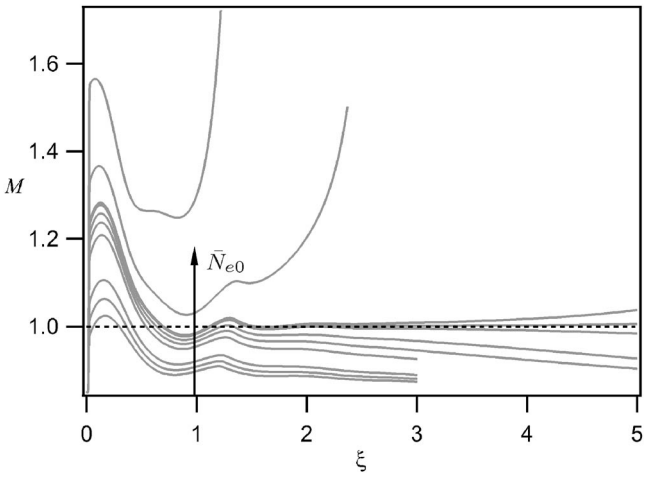

FIG. 9. The temporal development of M for various injected pulse sizes.

to reverse that trend; the avalanches increase in size and quickly merge, which will result in breakdown.

The key to achieving breakdown is the ability to raise M above unity through an increase in $\int_0^d \alpha(x)dx$. In Fig. 9 we plot M vs ξ for various injected pulse densities. In each case, M's initial value, M_0, is 0.85, but is instantaneously increased as a result of the initial electron avalanche. As successive avalanches develop, M rises and falls with the redistribution of ion density.

In all cases, M is made to exceed unity at least temporarily. However, in some cases, M falls below it again and a breakdown is not achieved—raising M temporarily above unity is not a sufficient criterion for breakdown. Furthermore, there are cases in which M exceeds unity, then drops below it, then increases again, resulting in breakdown. It is therefore clear that Townsend's classic breakdown condition, $M>1$, does not apply for undervoltage breakdown.

The Townsend model requires a positive gain over several avalanche generations in order for breakdown to be achieved. M is intended to be the ratio of the number of electron-ion pairs in one generation to the previous one. However, the quantity M varies *during* each ion avalanche transit. It is not surprising, then, that one can instantaneously achieve $M>1$, temporarily producing a lot of next-generation electrons, but not sustain that state for the entire ion transit. In such a case, the total number of charge carriers produced in the next generation might not be greater, and breakdown would not be achieved. Still, it seems obvious that if M never exceeds unity, a breakdown will never occur. We can thus say that $M(t)>1$ is a necessary but not sufficient condition for undervoltage breakdown.

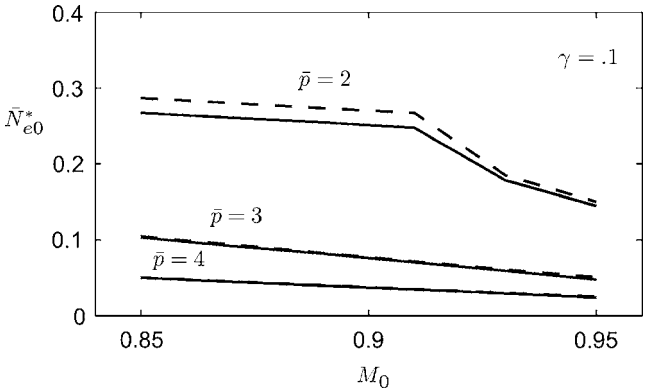

FIG. 10. Threshold curves for γ=0.1, $\bar{\mu}_+$=0.004 (solid), and $\bar{\mu}_+$=0.01 (dashed).

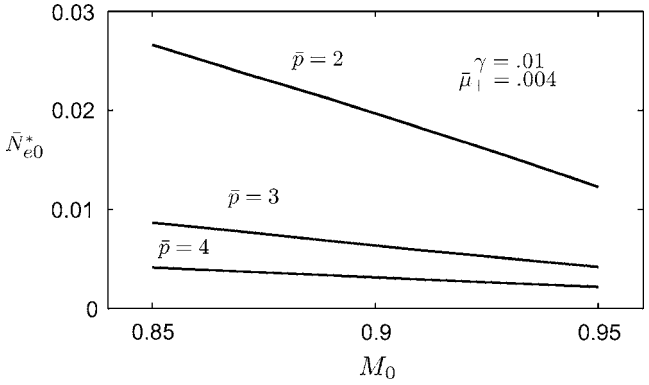

FIG. 11. Threshold curves for $\bar{\mu}_+$=0.004 and γ=0.01.

Such examination of the development of M allows us to address the question of threshold criteria. We designate an event as a breakdown if M trends upward over several ξ, then use the method of bisection to find the minimum $\bar{N}_{e0}$, a parameter we define as $\bar{N}^*_{e0}$, which will result in breakdown as a function of the other four input parameters.

Figures 10–12 contain threshold curves, plots of $\bar{N}^*_{e0}$ as a function of M_0 for various values of $\bar{p}$, γ, and $\bar{\mu}_+$.

IV. DISCUSSION

In Fig. 13, we plot $\bar{N}^*_{e0}$ as calculated from the experimentally measured threshold charge values displayed in Fig. 4. For each data point, we also plot the theoretically calculated value using published values for the Townsend ionization coefficients[12] for argon and assuming γ=0.1. The true secondary emission coefficient, and its dependencies on electric field and pressure, are highly dependent on surface conditions[16] and are not well known. That value of γ was chosen because it generates a good agreement between predictions and data, but it happens to fall within an expected range for these experimental conditions.

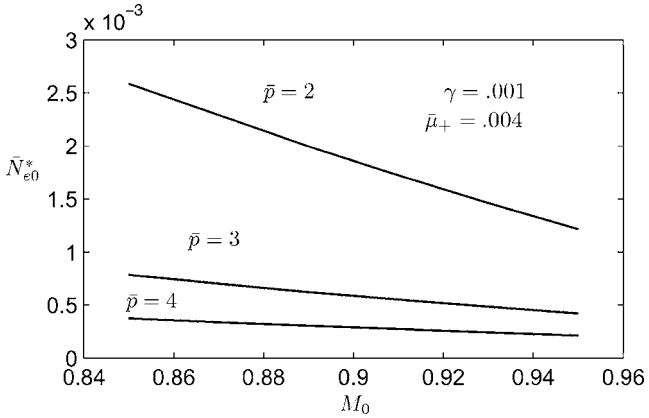

FIG. 12. Threshold curves for $\bar{\mu}_+$=0.004 and γ=0.001.

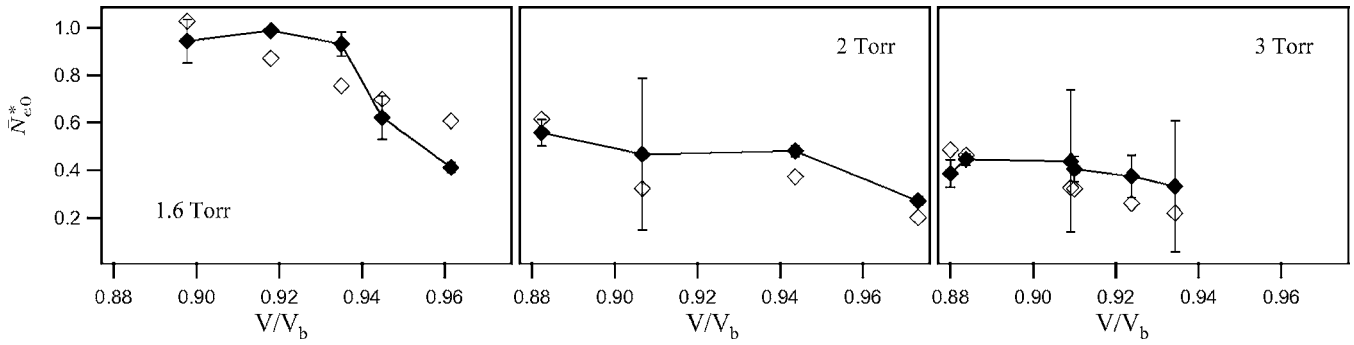

FIG. 13. $\bar{N}^*_{e0}$ as measured (solid) and calculated for γ=0.1 (open).

The dimensionless parameter $\bar{N}^*_{e0}$ represents the ratio of the critical injected charge to the charge on the electrodes and ranges within values on the order of 10^{-1} for these experimental conditions. In order to enhance ionization through a distortion of the applied electric field, we must provide sufficient charge to compete with that field. Ionization will amplify the injected charge, but at low gain the initial charge must still be a significant fraction of the applied charge. This is the fundamental difference between the phenomenon we are investigating, undervoltage breakdown through the Townsend mechanism at low gain, and breakdown in higher-gain devices, in which a single electron can start an avalanche that forms a streamer.

The trend of decreasing $\bar{N}^*_{e0}$ with increasing pressure ($\bar{p}$) is a demonstration of the importance of the α-process to undervoltage breakdown. At higher pressure, ionization is more field-limited than pressure-limited, and the system is more sensitive to increases in electric field such as those caused by the space-charge distortion. Since the critical E/p of $B/2$ ($\bar{p}\approx 2$) corresponds to a point on the Paschen curve that falls to the right of the minimum pd, we expect the pressure dependence of undervoltage breakdown to be monotonic over a reasonably wide parameter regime, until the gain becomes large enough that streamers form.

The relevance of the α process to undervoltage breakdown also explains the theoretically predicted dependence of critical pulse size on the secondary emission coefficient. Increasing γ increases $\bar{N}^*_{e0}$ because, at constant M_0, higher γ implies lower $\alpha_0 d$. Since undervoltage Townsend breakdown is achieved through the manipulation of gas amplification and not secondary emission, the phenomenon is more difficult to achieve when the amplification factor is reduced.

The weak dependence on ion mobility (Fig. 10) suggests that breakdown is determined during the first electron avalanche. The charge imbalance produced when the electrons leave the volume represents the largest electric field distortion that will occur during the breakdown process, raising M above unity and increasing ionization for subsequent avalanches. However, on the time scale of an electron avalanche, even the lightest ions are essentially stationary, and the mobility ratio is not relevant. Ionization increases and decreases in a complex fashion as further avalanches develop, but the general trend of growth or damping is established very early. The ion dynamics has only a minor effect on this process.

Using published data on the Townsend coefficients for argon,[12] we can calculate that $E/p=B/2$ (or $\bar{p}=2$), for the voltage range used in these experiments, corresponds to pressures ranging from 1.3 to 1.6 Torr. As discussed, these values represent approximate critical pressures below which undervoltage breakdown should not be possible, and indeed, no breakdowns were observed below 1.6 Torr.

V. CONCLUSIONS

We have experimentally and theoretically explored threshold conditions for undervoltage breakdown, the conditions under which a pulse of electrons will induce breakdown through the Townsend mechanism in a low-gain [$\exp(\alpha d) < 10^4$] discharge gap that is held below its breakdown voltage. From this investigation, we have gleaned the following physical insights into the phenomenon:

- Raising the breakdown parameter M above unity, at least temporarily, is necessary for undervoltage breakdown, but not sufficient.
- To achieve breakdown at low gain, the space-charge distortion must result from the magnitude of the injected pulse, so the injected charge must be significant when compared with the charge on the electrodes.
- Undervoltage breakdown is controlled by electron-impact ionization. It is thus easier as gain is increased, or as that process's sensitivity to electric field distortion is increased, such as through a reduction of E/p.
- Whether or not breakdown will occur is decided during, and immediately after, the transit of the first electron avalanche that results from the injected pulse. The phenomenon is therefore insensitive to ion mobility.

ACKNOWLEDGMENTS

The authors are thankful for support from the Program in Plasma Science and Technology at the Princeton Plasma Physics Laboratory. This work was supported by a DRDF grant from NASA-JPL.

[1] P. Fonte, V. Peskov, and F. Sauli, Nucl. Instrum. Methods Phys. Res. A **305**, 91 (1991).
[2] J. E. Cooley and E. Y. Choueiri, "Fundamentals of PPT discharge initiation: Undervoltage breakdown through electron pulse injection," in 39th Joint Propulsion Conference, Huntsville, AL, 2003, AIAA-2003–5027.
[3] K. Frank and J. Christiansen, IEEE Trans. Plasma Sci. **17**, 748 (1989).
[4] D. Šijačić, U. Ebert, and I. Rafatov, Phys. Rev. E **70**, 056220 (2004).

[5]D. Šijačić, U. Ebert, and I. Rafatov, Phys. Rev. E **71**, 066402 (2005).
[6]R. Kluckow, Z. Phys. **161**, 353 (1961).
[7]H. Raether, *Electron Avalanches and Breakdown in Gases* (Butterworth Co, Washington, D.C., 1964).
[8]M. F. Frechette, N. Bouchelouh, and R. Y. Larocque, "Laser-induced undervoltage breakdown in atmospheric N_2 correlated with time-resolved avalanches," in IEEE International Symposium on Electrical Insulation, Pittsburgh, PA, 5–8 June 1994.
[9]N. Sato and S. Sakamoto, J. Phys. D **12**, 875 (1979).
[10]P. Fonte, IEEE Trans. Nucl. Sci. **43**, 2135 (1996).
[11]A. Von Engel and M. Steenbeck, *Elektrische Gasentladungen* (Verlag Von Julius Springer, Berlin, 1932).
[12]Yu. P. Raizer, *Gas Discharge Physics* (Springer-Verlag, Berlin, 1997).
[13]D. Šijačić and U. Ebert, Phys. Rev. E **66**, 066410 (2002).
[14]R. Leveque, *Finite Volume Methods for Hyperbolic Problems* (Cambridge University Press, Cambridge, 2002).
[15]W. Press, S. Teukolsk, W. Vetterling, and B. Flannery, *Numerical Methods in C* (Cambridge University Press, Cambridge, 2002).
[16]A. V. Phelps and Z. Lj. Petrovic, Plasma Sources Sci. Technol. **8**, R21 (1999).